Journal of Hydrology 511 (2014) 786–799

Contents lists available at ScienceDirect

Journal of Hydrology

journal homepage: www.elsevier.com/locate/jhydrol

Impacts of climate change and vegetation dynamics on runoff in the mountainous region of the Haihe River basin in the past five decades

Huimin Lei [a], Dawen Yang [a,*], Maoyi Huang [b]

[a] State Key Laboratory of Hydroscience and Engineering, Department of Hydraulic Engineering, Tsinghua University, Beijing 100084, China
[b] Atmospheric Sciences and Global Change Division, Pacific Northwest National Laboratory, Richland, WA 99352, USA

ARTICLE INFO

Article history:
Received 20 May 2013
Received in revised form 28 January 2014
Accepted 10 February 2014
Available online 22 February 2014
This manuscript was handled by Konstantine P. Georgakakos, Editor-in-Chief, with the assistance of Michael Bruen, Associate Editor

Keywords:
Runoff
Climate change
Vegetation dynamics
Community Land Model
Haihe River basin

SUMMARY

Climate and atmospheric CO_2 concentration have changed significantly in the mountainous region of the Haihe River basin (in northern China) over the past five decades. In this study, a process-based terrestrial model, version 4 of the Community Land Model (CLM4), was used to quantify the spatiotemporal changes in runoff across the region, driven by the varying climate factors and CO_2 concentration. Overall, our simulations suggest that climate-induced runoff in this region display a decreasing trend since 1960. Changes in precipitation, solar radiation, air temperature, and wind speed account for 56%, −14%, 13%, and −5% of the overall decrease in annual runoff, respectively, although their relative contributions vary across the study area. The rise in atmospheric CO_2 concentration was determined to have a limited impact on runoff. A significant decrease in runoff in the southern and northeastern portions of the region is primarily attributed to decreasing precipitation, whereas decreasing solar radiation and increasing air temperature were the primary causes of a slight runoff increase in the northern portion. Our results also suggest that the magnitude of the decreasing trend may be greatly underestimated if the dynamic interactions of vegetation phenology and the environmental factors are not considered in the modelling, indicating the importance of including vegetation dynamics in the prediction of runoff trends in this region.

© 2014 Published by Elsevier B.V.

1. Introduction

There is a prevailing notion that climate has changed at an unprecedented rate over the past decades (Roderick and Farquhar, 2002; Yang and Yang, 2012; Piao et al., 2010; IPCC AR4). On the global scale, climate change has been shown to be the primary cause of changes in runoff (Shi et al., 2011; Gedney et al., 2006). However, changes in the hydrological cycle are not only a direct function of the climate, but are also regulated by vegetation dynamics, which also respond to the climate. Based on long-term observations and ecohydrological models, recent studies have already shown that vegetation plays an important role in modulating hydrological processes on various scales (Tague and Band, 2004; Ivanov et al., 2008; Yang et al., 2009; Donohue et al., 2012; Fatichi et al., 2012a,b; Shi et al., 2013).

Climate impacts the hydrological cycle via two different mechanisms: (1) the first mechanism consists of direct effects via water and energy exchanges. These effects have been investigated through hydrologic modelling at watershed to global scales (e.g., Cong et al., 2009; Dan et al., 2012; Wada et al., 2010). (2) The second consists of indirect effects via changes in vegetation dynamics (Piao et al., 2006; de Jong et al., 2011), which alter the hydrological cycle by way of such processes as canopy interception and leaf transpiration (Rodriguez-Iturbe, 2000). Generally, vegetation dynamics primarily include (1) photosynthesis, plant respiration, and stomatal physiology; (2) carbon allocation and translocation; (3) tissue turnover and stress-induced foliage loss; and (4) vegetation phenology (including the change in leaf area index (LAI)) (Fatichi et al., 2012a). Of these components, photosynthesis and stomatal conductance were incorporated into conventional land surface models or hydrological models earlier than other components (Pitman, 2003; Wang et al., 2009), to simulate the interconnected mechanisms of photosynthesis and leaf transpiration. However, simulations of vegetation phenology and its related processes are usually neglected in conventional hydrological models by prescribing known vegetation phenology information such as remotely sensed LAI values. This treatment failed to simulate the response of vegetation phenology to the changing climate, leaving the effect of climate on the hydrological cycle via the impact on vegetation phenology unknown. In recent years, an increasing number of studies have begun to include vegetation dynamics, including all of the components mentioned above, in ecohydrological, land surface, and dynamic vegetation models to

* Corresponding author. Tel.: +86 10 62796976; fax: +86 10 62796971.
E-mail address: yangdw@tsinghua.edu.cn (D. Yang).

http://dx.doi.org/10.1016/j.jhydrol.2014.02.029
0022-1694/© 2014 Published by Elsevier B.V.

assess the integrated impacts of climate on the hydrological cycles via both effects (Tague and Band, 2004; Ivanov et al., 2008; Li and Ishidaira, 2012; Fatichi et al., 2012a,b; Shen et al., 2013; Davie et al., 2013; Murray et al., 2013) and have demonstrated that neglecting vegetation dynamics in these models may lead to potentially large uncertainties in hydrological simulations.

In water-limited regions, attributing the trend in runoff to the changing climate and anthropogenic factors is a topic that is important for future water resources planning and management decisions to ensure sustainable water resources utilisation. Partitioning the effects of climate change and human activities is usually performed with the aid of hydrological models (Ma et al., 2010). One basic assumption in this type of study has been that the change in runoff caused by climate change during the study period can be reproduced using a hydrological model. The trend in runoff caused by human activities can be then defined as the difference between the observed runoff and the "natural runoff" simulated by the hydrological models. Therefore, a critical aspect is that a hydrological model can respond realistically to the changing climate and can capture the trend in the natural runoff, particularly during a period when vegetation data are unavailable. However, although vegetation dynamics have been already incorporated in ecohydrological models exploring the causes of changes in river discharge (e.g., Gerten et al., 2008), the impacts of vegetation dynamics on the simulation of runoff trends still merits additional investigation.

The Haihe River basin is located in northern China (Fig. 1). Its total area measures approximately 318,000 km^2, and its mountainous area measures approximately 189,000 km^2. The amount of water resources per capita is only 305 m^3 year^{-1}, which is only 1/7 of the national average (Haihe River Commission, 2013). Water resource shortages are becoming a critical challenge in economic development of this region. In the mountainous region of the Haihe River basin, runoff is only 12% of the mean annual precipitation (Yang et al., 2007), while it is an indispensable water source of municipal and industrial uses in large cities (e.g., Beijing, Tianjin, Shijiazhuang) and supplies water for irrigating croplands in the plain area of the downstream basin. One important motivation for studying the effects of climate change on the runoff trend in the region is that the region is a typical semi-humid one with a significant decreasing trend in streamflow (Yang and Tian, 2009). Recently, there have been quantitative efforts to attribute the decline in runoff in selected watersheds in this region in the past five decades to climate change and human activities (Ma et al., 2010; Jia et al., 2012; Wang et al., 2012; Bao et al., 2012; Peng et al., 2013). However, these studies are incomplete to a certain extent due to their failure to consider feedbacks between the hydrological cycle and vegetation, and their attribution of the responses of runoff to individual climate factors (e.g., solar incident radiation, air temperature, wind speed, and CO_2 concentration), given that these factors have changed significantly over the past five decades (Zheng et al., 2009). As a result, the role of climate change in runoff trends over the past half century, particularly the contribution of the rising CO_2 concentration and the indirect effects of climate change through changes in vegetation dynamics, is still unclear.

To address these issues, this study was designed to investigate the manner in which climate factors, including precipitation, solar radiation, air temperature, humidity, wind speed, and atmospheric

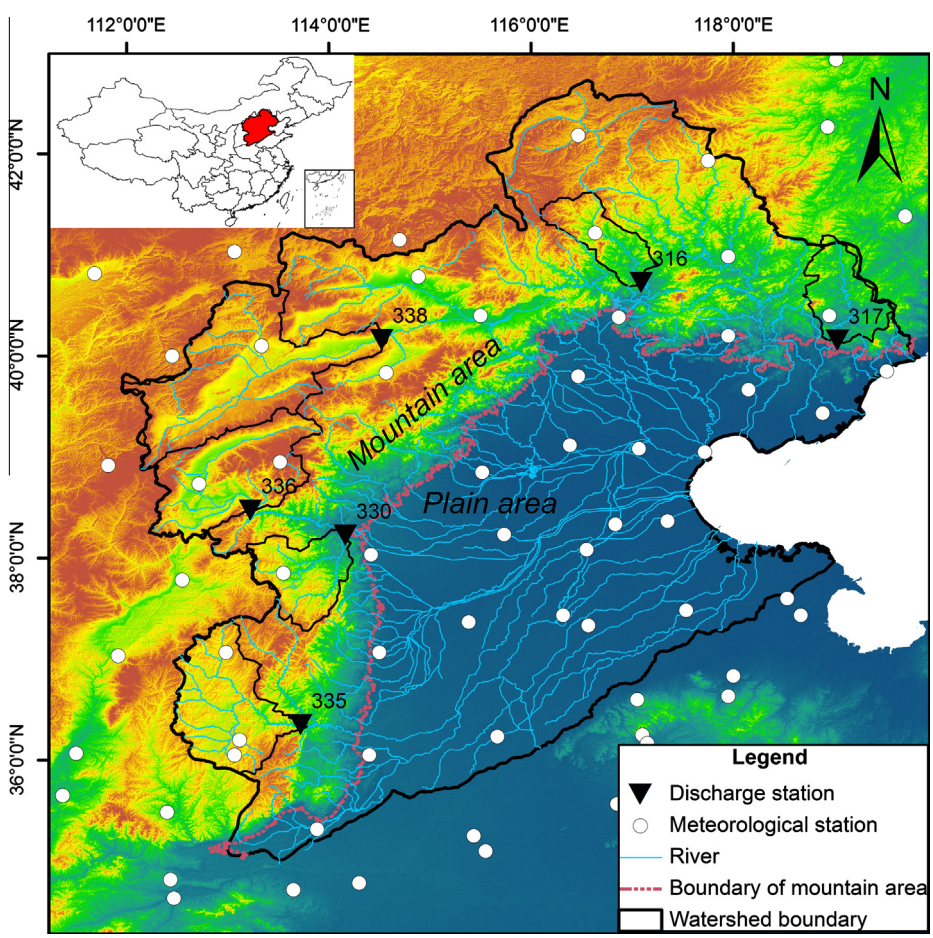

Fig. 1. Study area and the station locations.

CO_2 concentration have altered runoff in the mountainous region of the Haihe River basin over the past five decades by considering both the direct and indirect effects of changing climate and to identify the dominant climate factors that impacted the changes in runoff. We selected version 4 of the Community Land Model (CLM4), which is capable of representing the necessary biogeophysical and biogeochemical processes, as discussed in Section 2, to simulate changes in the annual runoff in the period of 1960–2010. Based on the simulations, we quantified the relative contributions of the climate factors to historical changes in runoff. In particular, we emphasised the impacts of dynamic vegetation phenology on runoff simulations, which have not been fully considered in conventional hydrological models.

2. Model description and experimental design

2.1. Model description

CLM4 simulates the land surface biophysical (i.e., water and energy budgets) and biogeochemical processes (i.e., carbon and nitrogen cycles). Its hydrological components include the canopy hydrology (interception, throughfall, and drip), snow hydrology (snow accumulation and melt, compaction, water transfer between snow layers), soil hydrology (surface runoff, infiltration, redistribution of water within the column, sub-surface drainage, and groundwater), and evapotranspiration. Evapotranspiration is the link between the water, energy, and biogeochemical cycles. It is directly driven by the gradient of specific humidity and controlled by a series of resistances parameters between the leaf interior and the atmosphere, such as leaf stomatal resistance, aerodynamic resistance, and boundary layer resistance. Subgrid spatial heterogeneity is represented as a nested hierarchy in which grid cells are composed of multiple landunits (i.e., glacier, wetland, vegetated land, lake, and urban). The cells of vegetated land are further decomposed into 16 plant function types (PFTs) (Bonan et al., 2002) (e.g., temperate needleleaf evergreen tree, temperature broadleaf evergreen shrub, C3 grass, cropland) and bare ground, if present. Each PFT differs in its optical properties, root distribution parameters, aerodynamic parameters (e.g., the ratio of momentum roughness length to canopy top height), and photosynthetic parameters.

CLM4 (and its previous versions) has been evaluated in previous studies using eddy-covariance flux measurements (Stöckli et al., 2008; Li et al., 2011; Hou et al., 2012), small watersheds (Li et al., 2011; Huang et al., 2013), and soil moisture sampling data (Wang and Zeng, 2011) but has been primarily used for global and regional studies (e.g., Wang and Zeng, 2011; Shi et al., 2013). By comparing the observed river discharge and observation-based evapotranspiration product, CLM4 is able to realistically reproduce the trend in annual river flow (Shi et al., 2011) and interannual variation in ET (Shi et al., 2013), respectively. A comprehensive description of CLM4 can be found in Oleson et al. (2010) and Lawrence et al. (2011). The formulations for describing runoff, river discharge, and carbon–nitrogen cycles, which are closely tied to this study, are briefly described below.

2.1.1. Runoff generation and river routing

The TOPMODEL-based schemes are adopted in CLM4 to represent the generation of runoff. The surface runoff, q_{over}, is expressed as

$$\begin{cases} q_{over} = f_{sat} q_{liq,0} + (1 - f_{sat}) \max\left[0, (q_{liq,0} - q_{infl,max})\right], \\ f_{sat} = f_{max} \exp(-C_s f_{over} z_\nabla) \end{cases} \quad (1)$$

where $q_{liq,0}$ is the liquid precipitation reaching the ground plus any melt water from snow; $q_{infl,max}$ is the maximum soil infiltration capacity, z_∇ is the water table depth, and f_{max}, C_s, and f_{over} are model parameters. The subsurface runoff is parameterised as follows:

$$q_{drai} = q_{drai,max} \exp(-f_{drai} z_\nabla) \quad (2)$$

where $q_{drai,max}$ and f_{drai} are model parameters. Note that the parameters in the TOPMODEL-based scheme are fixed as constant (i.e., $C_s = 0.5$, $f_{over} = 0.5\ m^{-1}$, $q_{drai,max} = 5.5 \times 10^{-3}\ mm\ s^{-1}$ and $f_{drai} = 2.5\ m^{-1}$) in CLM4, except for the spatially varying f_{max} derived from digital elevation models (DEMs). These constant values were determined though sensitivity analyses by comparing the simulated global runoff to observed global runoff (see Table 1 in Hou et al. (2012) for details).

The stream discharge is simulated by the River Transport Model (RTM) in CLM4 (Branstetter and Erickson, 2003; Oleson et al., 2010). The RTM was developed to route total runoff generated using CLM4. In the RTM, the change in stream water storage (S) within an RTM grid cell is given by

$$\frac{dS}{dt} = \sum F_{in} - F_{out} + R \quad (3)$$

where $\sum F_{in}$ is the sum of inflows from neighboring upstream grid cells, F_{out} is the outflow to the downstream grid cell, and R is the total runoff generated by CLM4 at the cell. F_{out} is parameterized using the equation

$$F_{out} = \frac{v}{d} S \quad (4)$$

where v is the effective water flow velocity and d is the distance between centers of neighboring RTM grid cells. Currently, v is assumed to be spatially constant (i.e., $0.35\ m\ s^{-1}$) in CLM4.

2.1.2. Carbon and nitrogen cycles

CLM4 includes a fully prognostic treatment of the terrestrial carbon and nitrogen cycles (CN) to simulate the dynamic vegetation phenology (specified in this study as the leaf area index, stem area index, and vegetation height). The CN model stems from the ecosystem model, Biome-BGC (version 4.1.2) (Thornton and Rosenbloom, 2005; Oleson et al., 2010), which prognostically simulates carbon and nitrogen state variables in the form of vegetation, litter, and soil organic matter. The prognostic vegetation phenology is used by the biophysical component in CLM4, which calculates the soil temperature and moisture and feeds these values back to the CN model. When the CN model is turned off, only photosynthesis and the control of leaf transpiration by leaf stomatal resistance are simulated, whereas the vegetation phenology should be prescribed. Crops are treated as unmanaged grass using the biophysical and biogeochemical parameters of C3 grass without any farm management.

2.2. Data acquisition and post-processing

To run CLM4, two types of data were needed: atmospheric forcing data and land surface parameters. The atmospheric forcing data included the climate, nitrogen deposition, aerosol deposition, and CO_2 concentration, as presented in Table 1. Due to the lack of high-resolution atmospheric nitrogen and aerosol deposition datasets, global $0.5° \times 0.5°$ data were used to enable the model to provide a best realistic estimate. The land surface parameters included the types of landunits, plant function types, and soil texture, which are listed in Table 1.

Climate data were obtained from 73 Chinese Meteorological Administration stations located in and around the Haihe River basin (Fig. 1). Observations from the stations included the daily precipitation; daily average, maximum, and minimum air temperature; daily average relative humidity; daily sunshine duration; and daily average wind speed. The daily observed data were

Table 1
Environmental driver datasets used in the simulations from 1960 to 2010.

Data type	Source	Time step	Original spatial resolution	Data used for model spinup	Note
Climate	China Meteorological Data Sharing Service System (http://www.cdc.cma.gov.cn)	3-hourly	73 stations	Repeated 1960–1969	Historical observed data
Nitrogen deposition	Dentener et al. (2006)	Yearly	0.5° × 0.5°	Average from 1950 to 1959; NHx and NOy, used for N cycle in the CN sub-model	NHx and NOy
CO_2 concentration	Global View (http://www.esrl.noaa.gov/gmd/ccgg/globalview/co2/co2_intro.html)	Monthly	0.5° × 0.5°	Average from 1950 to 1959; used for the C cycle	Latitudinal varying boundary layer CO_2 concentrations
Aerosol deposition	NCAR (default from NCAR at http://www.cesm.ucar.edu/models/cesm1.0)	Monthly	0.5° × 0.5°	Averaged from 1950 to 1959; used for snow sub-model	Simulated by the Community Atmospheric Model (CAM)
Landuse type	Environmental & Ecological Science Data Center for West China (http://www.westdc.westgis.ac.cn/)	One-time	30 m × 30 m		Remotely sensed data in 2000
Soil texture	Shangguan et al. (2012)	One-time	0.00833° × 0.00833°		Sand and clay percent
Maximum saturated fraction (f_{max})	Li et al. (2013a,b)	One-time	0.05° × 0.05°		Parameter used in calculating surface runoff
Organic soil density	NCAR (default from NCAR at http://www.cesm.ucar.edu/models/cesm1.0)	One-time	5′ × 5′		Parameter used for calculating soil's thermal and hydraulic properties
Urban parameters	Jackson et al. (2010)	One-time	–		Parameters used for urban sub-model
Soil color	NCAR (default from NCAR at http://www.cesm.ucar.edu/models/cesm1.0)	One-time	0.5° × 0.5°		Parameters used for calculating soil albedo
VOC emission factor	NCAR (default from NCAR at http://www.cesm.ucar.edu/models/cesm1.0)	One-time	0.5° × 0.5°		Parameters of MEGAN BVOC (a biogenic volatile organic compounds sub-model)

downscaled to 3-hourly intervals using the empirical methods of Lei et al. (2013) for input to CLM4. Briefly, the daily precipitation was downscaled by assuming an isosceles-triangle distribution of the hourly values; the daily temperature was downscaled to hourly temperature using a sinusoidal function; the daily sunshine duration was used to estimate hourly solar incident radiation using a simple model (Yang and Koike, 2005); and the hourly relative humidity and hourly wind speed were assumed to be equal to their daily average values. We then we used an angular distance weighting method (Yang et al., 2004) to interpolate between the station data to develop regional gridded values at a 0.05° × 0.05° resolution. Elevation corrections were applied to interpolate the air temperature and atmospheric pressure using algorithms of Yang et al. (2004).

The soil data were those of Shangguan et al. (2012), which represent the soil textures of the surficial (0–30 cm) and underlying (30–100 cm) soil layers. For compatibility with the soil layers CLM4 (soil depth is set at 380 cm in CLM4), the upper and lower soil textures were assigned to the upper five (i.e., 0–29 cm) and lower five layers (i.e., 29–380 cm) in CLM4, respectively, by assuming that the soil texture below 100 cm is the same as that of the interval between 30 and 100 cm.

The land cover data from the year 1985 were obtained from the Environmental & Ecological Science Data Center for West China (EESD) (http://westdc.westgis.ac.cn) (Liu et al., 2005). This dataset contained the highest resolution land cover data available for China. The land classification system of the EESD data was not consistent with that of CLM4. Therefore, a mapping rule to convert the EESD land cover types to CLM4 classifications was developed for the study region based on the 1:4,000,000 vegetation map of China (http://westdc.westgis.ac.cn), as shown in Table 2. The 30-m EESD data were aggregated to a resolution of 0.05° to obtain the area fractions of each CLM land cover/PFT types. The monthly leaf area index (LAI) data from 1982 to 2010 were obtained from a dataset that was a fusion of advanced very high resolution radiometer (AVHRR) data and moderate resolution imaging spectroradiometer (MODIS) data (Liu et al., 2012). The LAI data were used to prescribe seasonal variations in the LAI in the simulations for evaluating the impact of the simulation of vegetation phenology (described below). The flow direction data at a resolution of 0.0625° developed by Wu et al. (2012) were used as inputs to the RTM.

2.3. Experimental design

The relative contributions of each factor to the trend in annual runoff were calculated following the approach used in previous studies (Lucht et al., 2002; Piao et al., 2012; Shi et al., 2011). Therefore, eight simulations were performed, as summarised in Table 3. In these simulations, CLM4 was run for the period of 1960–2010 (Table 1) at a 0.05° resolution (approximately 5 km × 5 km in this region). To obtain the initial variables in these simulations, the model (with CN model turned on) was spun up by cycling the climate forcing over the period 1950 to 1959 using the input data in Table 1 until steady-state criteria for both the carbon and water cycles were satisfied. These criteria were as follows: the regional mean total ecosystem carbon values of corresponding months of two repeated 1950–1959 runs differed by less than 1 gC m^{-2}; and the corresponding monthly values of the regional mean volumetric soil water content, net ecosystem exchange, net ecosystem production, soil temperature, and water table depth of the two climate forcing cycles differed by less than 1%.

In simulations S1–S7, the model was run with the CN model "turned-on" to allow for feedbacks between the vegetation dynamics and environmental factors. In simulations S1–S6, one of the

Table 2
Mapping rules for converting from EESD land use types to CLM4 plant functional types and landunits in the Haihe River basin.

Land use type in EESD	Plant functional type or landunit in CLM4	Note
Paddy filed Dry cropland	Crop1 (i.e., cropland without irrigation)	Assuming that cropland in this region is not irrigated
Dense tree (cover > 30%) Sparse tree (cover: 10–30%) Other forest (e.g., orchard)	Broadleaf deciduous tree – temperate	No other tree PFTs in this region according to China's vegetation map
Shrubland	Broadleaf deciduous shrub – temperate	No other shrub PFTs in this region according to China's vegetation map
Dense grassland (coverage > 50%) Moderate grassland (coverage: 20–50%) Sparse grassland (coverage: 5–20%)	C_3 grass	Assuming no C_4 grasses because grassland is dominated by C_3 grasses in the region (Edwards et al., 2010)
River and channel	Bare soil	River and channel are not represented as CLM4's landunits, thus they are assigned to bare soil because rivers and channels usually dry up in the basin
Lake Reservoir	Lake	
Permanent ice and snow	Glacier	
Beach and shore Bottomland	Bare soil	
City Village Other built-up land (e.g.: oil field, road, airport)	Urban	
Sandy land Gobi Salina	Bare soil	
Swampland	Wetland	
Bare soil Bare rock Other unused land (e.g.,: alpine desert and tundra)	Bare soil	

environmental factors was held constant (i.e., allowing for seasonal variability but no interannual variability; mean values at the same time coordinate of every year were used to represent the seasonal variability), and the remaining factors were allowed to vary with time. In simulation S7 (i.e., the baseline simulation), all of the factors were allowed to vary with time, and thus this simulation provided the best and most realistic estimate of the runoff. The impact of each environmental factor was then defined as the difference between the results of simulation S7 and those of the corresponding simulation of interest (i.e., S1–S6). To explore the impacts of dynamic vegetation phenology on runoff, an additional simulation (S8) was run using the monthly cycle of LAI based on 1985 satellite data (with the CN model turned off). In other words, vegetation with all the carbon pools in simulation S8 is static rather than dynamic. Therefore, the difference in runoff between simulations S7 and S8 is attributed to the year-to-year difference in vegetation phenology, either simulated by the CN model (i.e., S7) or prescribed (i.e., S8).

Table 3
Experimental design of sensitivity analysis.

Simulation	Description	Individual factor	If CN sub-model turned on
S1	Constant precipitation	Precipitation: S7–S1	Yes
S2	Constant air temperature	Air temperature: S7–S2	
S3	Constant solar radiation	Solar radiation: S7–S3	
S4	Constant relative humidity	Relative humidity: S7–S4	
S5	Constant wind speed	Wind speed: S7–S5	
S6	Constant yearly CO_2	CO_2: S7–S6	
S7	All factors were time-varying	All factors	
S8	All factors were time-varying	All factors	No (prescribed with monthly cycle of LAI in 1985)

The contribution of each environmental factor to the overall trend in annual runoff was calculated by dividing the trend calculated from its corresponding simulation (i.e., S1–S6 minus S7) by the trend from S7. It is worth mentioning that the trend of S7 also received contributions from transient nitrogen deposition and aerosol deposition. Because the resolutions of the nitrogen and aerosol deposition datasets covering our study area were too coarse, we did not analyse the impacts of nitrogen and aerosol deposition on the trends in runoff. Rather, we included them in all of the simulations and treated them as large scale background inputs.

To evaluate the uncertainties caused by hydrological parameters and modelling of the LAI, we designed three supplementary simulations spanning the period 1982–2010 because only remotely sensed LAI data from this period were available (details are listed in Table 4). In these simulations, the CN model was turned off and the LAI used was prescribed with the remotely sensed monthly LAI from 1982 to 2010. In simulations D1 and D2, all of the parameters were the default values in CLM4. Because the runoff simulation was found to be most sensitive to the three hydrological parameters, f_{drai}, $q_{drai,max}$, and f_{over} (Huang et al., 2013), the three parameters were tuned subjectively in simulation D3. As no vegetation equilibrium status was expected in these simulations (vegetation status was prescribed using the remotely sensed LAI data), the model was run for only six years to eliminate the influence of arbitrary initial values on the runoff simulations. Based on simulations D1 and D2, the calculated contribution of precipitation to the trend in annual runoff was for the case in which the response of LAI to the changing climate was not considered and was a result of conventional hydrological modelling, which neglects the feedback of vegetation phenology to a changing climate.

Table 4
Experimental design for evaluating the uncertainties.

Simulation	Description	Parameters
D1	All factors were time-varying	Default parameters in CLM4 (i.e., f_{over} = 0.5 m^{-1}, $q_{drai,max}$ = 5.5 × 10^{-3} mm s^{-1} and f_{drai} = 2.5 m^{-1})
D2	Constant precipitation	Default parameters in CLM4 (f_{over} = 0.5 m^{-1}, $q_{drai,max}$ = 5.5 × 10^{-3} mm s^{-1} and f_{drai} = 2.5 m^{-1})
D3	All factors were time-varying	f_{over} = 4.0 m^{-1}, $q_{drai,max}$ = 3.0 × 10^{-5} mm s^{-1} and f_{drai} = 4.0 m^{-1}

In all of the simulations, we assumed that forests and grasslands were not disturbed by human activities, such as logging and grass grazing because such information was not readily available. Moreover, we did not consider irrigation of croplands because most of the croplands in the mountainous region are rain-fed (approximately 6.3% of the areas were irrigated (Sun and Ren, 2013)).

2.4. Evaluation data

The observed annual river discharge and three remote sensing products were used to evaluate the model (Table 5). A comparison of river discharge in the region was very difficult. Theoretically, the gauge stations near the river mouths should be selected to match the spatial representativeness of the climate forcing data. However, the river discharge at the river mouth in the plain area is dramatically disturbed by human activities, such as water withdrawal and reservoir regulation (Liu and Xia, 2004), and therefore the corresponding discharge data are not appropriate for use in evaluating the simulated river discharge, as the model does not consider the impacts of human activity.

Instead, the gauge stations located at the outlets of upstream mountainous tributary watersheds of the Haihe River basin were selected as validation datasets in this study. According to Yang and Tian (2009), the streamflows in most of the rivers in the mountainous region can be treated as approximately "natural" before 1980 because the impacts of human activity on streamflows were relatively small, Due to rapid increases in croplands and population starting in 1980 (Bao et al., 2012), the observed streamflows were modified by anthropogenic effects after 1980.

Due to the sparsity of meteorological stations (Fig. 1) in the mountainous region, there is substantial uncertainty in the station-derived gridded climate forcing data. Therefore, we performed additional screening to include only the gauge stations where there was at least one meteorological station in the corresponding watershed area. The delineations of source areas provided by the dataset of Wu et al. (2012) should be similar to the survey-based source areas of the gauge stations, as the dataset is subject to errors embedded in its source DEMs from satellite observations (i.e., the Shuttle Radar Topography Mission). The six gauge stations that passed the screening are shown in Fig. 1. The observed river discharge data at these stations from 1960 to 1980 were used to evaluate the simulated river discharge in simulation S7, and the observed discharge data from 1988 to 2005 were used as a reference in simulations D1–D3.

The remotely sensed gross primary production (GPP), ET and leaf area index (LAI) data were used to evaluate the temporal variability of the simulated variables. The MODIS and AVHRR based products from the University of Montana were used to validate the GPP and ET, respectively (Zhao et al., 2005, 2006; Zhang et al., 2010). However, we note that both datasets were developed using modelling approaches that fused the remote-sensing products with global daily meteorological datasets and therefore should be considered less reliable than the LAI.

3. Results and discussion

3.1. Model validation

Table 6 lists the statistics of the comparison between the simulated and observed annual mean river discharges in these small basins. Overall, the Nash–Sutcliffe coefficients (NSEs) of these hydrological stations were not high. The NSEs of three of these stations were even negative, which means that the observed mean is a better predictor than the model simulation. These results were not surprising because the NSE uses the observed mean as baseline (Gupta et al., 2009), and there were large biases between the mean annual discharges of the simulations and observations (possible explanations for the relatively low NSE are discussed in Section 3.5). However, the NSE value rose to 0.7 if we averaged the discharge over all of the small basins, which implies that the model involved a relatively large uncertainty at small scales but exhibited generally good performance at the relatively large scale at which our analysis was performed. If we focus on the interannual variability of the runoff, the simulated and observed variability are consistent, as indicated by high correlation coefficients. Fig. 2a compares the observed and simulated trends in annual river flow over the period 1960–1980 for the 6 rivers. The simulated and observed trends in river flow are significantly correlated (significance level = 10%), and the simulation captured a relatively high fraction of the observed variance (R^2 = 0.61). However, the average slopes of the annual runoff were −0.42 and −0.22 m^3 s^{-1} year^{-1} in the observation and CLM4 simulation, respectively (Fig. 2b). The possible explanation for the disparity are that: (1) the observed slope of annual runoff received contribution from such human activities as water withdrawal during the simulation period, even though these withdrawals may have been relatively small; (2) there were uncertainties in the runoff simulation which are discussed in more detail in Section 3.5. Nevertheless, the comparisons suggest that the CLM4 model simulations are generally valid for evaluating the mechanisms controlling the changes in stream flow at relatively large scales.

Table 5
Observed data and remote sensing products used for model evaluation.

Data and type	Time	Spatial resolution	Source
Runoff, observed	Yearly from 1960 to 2005	Six stations in the upper reach of the river, see Fig. 1	Bureau of hydrology
Gross primary production, remote sensing-based product (MODIS)	Monthly, from 2000 to 2010	0.05° × 0.05°	Zhao et al. (2005, 2006)
Evapotranspiration, remote sensing-based product	Monthly, from 1983 to 2006	0.073° × 0.073° (about 8 km × 8 km)	Zhang et al. (2010)
Leaf area index, remote sensing product	Half-month from 1982 to 1999, and 8-day from 2000 to 2010	0.073° × 0.073°	Liu et al. (2012)

Table 6
Statistics of the comparisons of the river discharge.

Gauge number	Source area of the gauge (km^2)	Observed mean annul runoff ($m^3 s^{-1}$)	Simulated mean annul runoff ($m^3 s^{-1}$)	Nash–Sutcliffe coefficient between the simulated and observed annual river discharge	Correlation coefficient between the simulated and observed annual river discharge	The number of meteorological stations in the drainage area of the gauge
335	11,250	25.8	25.3	0.66	0.93	3
330	6420	20.0	16.3	0.67	0.95	1
336	11,936	18.8	36.3	−2.7	0.93	2
338	25,533	18.4	15.8	0.33	0.66	1
316	4266	8.9	0.5	−3.5	0.63	1
317	5060	27.6	14.8	−0.05	0.96	1
Average		19.9	18.2	0.70	0.87	

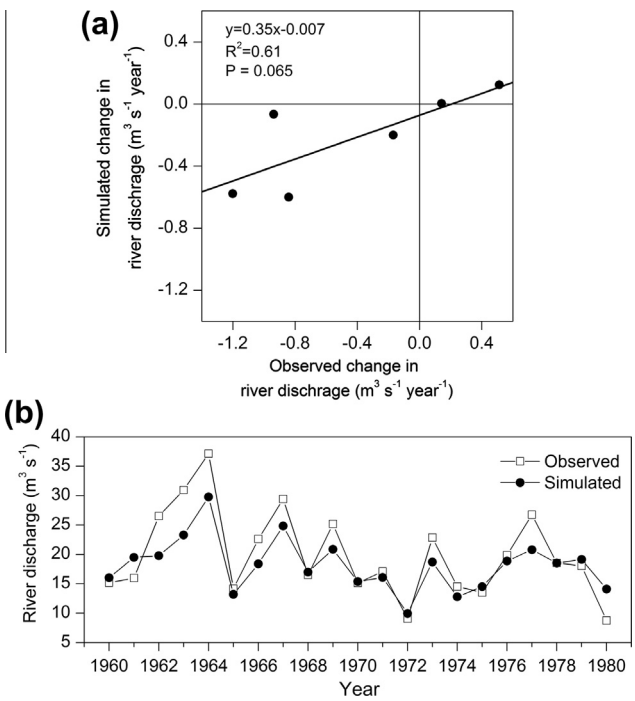

Fig. 2. (a) Comparison of simulated and observed change in flow in the 6 rivers during the period 1960–1980; (b) interannual variations in average simulated and observed runoff in the 6 rivers.

Fig. 3 shows a comparison of the annual mean LAI anomaly from 1982 to 2010. The mean annual LAI simulated using CLM4 was 1.3 ± 0.17 $m^2 m^{-2}$, which was much higher than the remotely sensed LAI (0.6 ± 0.05 $m^2 m^{-2}$). Moreover, the interannual variability in the simulated LAI was higher than that of the remotely sensed LAI, suggesting that the simulated vegetation phenology was more sensitive to the variations in environmental factors than the actual vegetation phenology. The inconsistency between the simulated and remotely sensed LAIs may be explained as follows: First, CLM4 simulates the potential vegetation status by spinning up the model to reach equilibrium forced by the environmental factors, in which case any impacts of human-induced disturbances are ignored. However the remotely sensed LAIs are considered representative of the actual status of the vegetation. Second, the biophysical canopy parameters or certain underlying parameterisations (e.g., Tan et al., 2010), which are sensitive to the simulated canopy structure in the CN model, are specified based on observations from other regions available when the model was developed and therefore may be not representative of the vegetation in this region. Similar systematic high biases in simulated LAIs have also been reported in previous studies using process-based models when model parameters and/or structures were not appropriate (e.g., Sakaguchi et al., 2011; Tan et al., 2010).

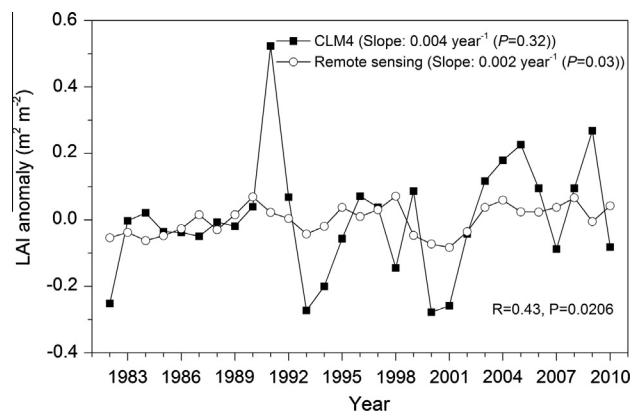

Fig. 3. Interannual variations in LAI anomaly from 1982 to 2010.

Figs. 4 and 5 show comparisons of the GPP and ET, respectively. The mean annual GPP simulated using CLM4 was 697 gC m^{-2} $year^{-1}$, i.e., higher than the MODIS GPP (539 gC m^{-2} $year^{-1}$). This disparity was primarily because the high bias in the simulated LAI propagates to the simulated GPP, although MODIS GPP may also be biased in this region (Mao et al., 2012). The mean annual ET simulated using CLM4 was 470 mm, close to the remotely sensed ET (429 mm). This finding implies that the systematic bias from the magnitude of the simulated LAI may affect the carbon cycle simulations more than do the water cycle simulations. However, as the ET is a major component of water balance in the region (mean annual precipitation during this period was 483 mm), a small bias in the ET simulation will also cause a large error in the simulated magnitude of the runoff. In terms of the trends in the annual time series, both the simulated GPP and ET are consistent with the remotely sensed products. Moreover, the interannual variability in the simulated GPP and ET is consistent with that of the MODIS GPP and remotely sensed ET, respectively. Overall, CLM4 is capable of reproducing reasonable interannual variability and trends in the GPP and ET, suggesting that the model was capable of capturing the mechanisms controlling land–atmosphere water and carbon exchange in this region. However, the poor agreement between the LAI trend and its interannual variability in simulation S7 and the satellite derivation suggests that the mechanisms controlling the LAI changes were not fully captured by CLM4. The uncertainty in the impact of LAI simulation on runoff is discussed in more detail in Section 3.5.

3.2. Temporal trends in climate forcing

The temporal trends in climate forcing were analysed to develop an understanding of their historical changes. The spatially averaged trends in climate forcing during the period of 1960–2010 are listed in Table 7. Of these factors, the air temperature and

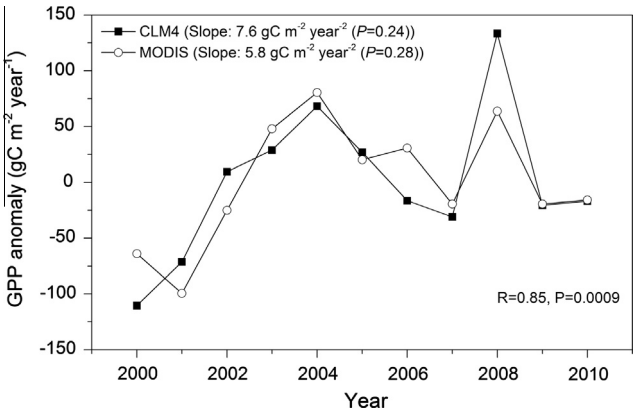

Fig. 4. Comparison of the simulated and MODIS GPP anomaly.

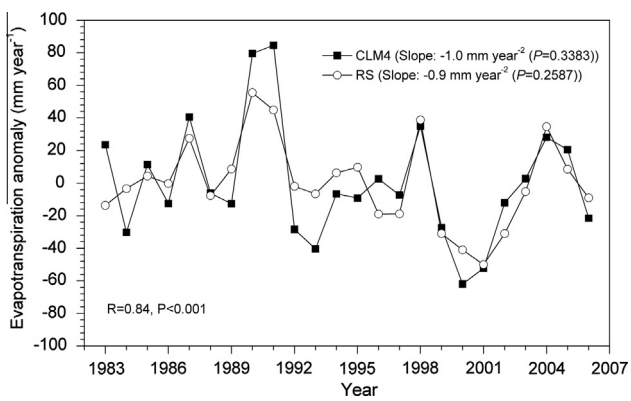

Fig. 5. Comparison of the simulated and remote sensing evapotranspiration.

atmospheric CO_2 concentration increased significantly ($P < 0.05$), whereas the solar incident radiation and wind speed decreased significantly ($P < 0.05$). Precipitation also exhibited a decreasing rate, although the trend is not significant (significance level = 0.05). The trend in relative humidity is not significant. The results of our analysis are consistent with those of previous studies (Zheng et al., 2009; Wang et al., 2011), suggesting that the trends in the climate factors were complex in terms of either their directions or their magnitudes of change.

3.3. Temporal and spatial changes in runoff

The simulated spatially averaged runoff across the entire mountainous region of the Haihe River basin displayed a significant ($P < 0.05$) decreasing trend from 1960 to 2010, with a rate of -0.50 mm year^{-2} (Fig. 6). This result was consistent with those of previous studies, in which it is reported that the simulated annual runoff decreased due to changes in climate forcing. For example, Ma et al. (2010) reported that the change in flow into Miyun Reservoir (located in the northern Haihe River basin) induced by climate change was -1.2 mm year^{-2} from 1956 to 2005; Wang et al. (2012) reported that climate variability accounted for a decreasing trend in annual runoff from 0.7 mm year^{-2} (Basin No. 316 in our study) to 2.5 mm year^{-2} (Basin No. 336 in our study) from 1957 to 2000 in 4 small basins in the Haihe River basin.

We further investigated the relative contributions of climate forcing to the spatially averaged runoff (Table 8). Among these factors, precipitation played a dominant role in the decrease of simulated runoff. Although the decrease in annual precipitation was not significant, the slight decrease in precipitation was amplified in the simulated runoff ($P < 0.05$).

Table 7
Summary of the trends in climate forcing.

Climate forcing	Annual mean	Trend (*P*-value)
Precipitation	483 mm	-1.27 mm year^{-1} (0.0836)
Air temperature	7.325 °C	**+0.038** °C year^{-1} (6.06E−10)
Solar radiation	181.9 W m^{-2}	**−0.3** W m^{-2} year^{-1} (1.53E−10)
Relative humidity	66%	-0.0057 year^{-1} (0.81)
Wind speed (at 10-m height)	2.0 m s^{-1}	**−0.014** m s^{-1} year^{-1} (2.72E−14)
Atmospheric CO_2 concentration	324 ppm	**+1.3** ppm year^{-1} (2.74E−45)

Bold text indicates that the trend is statistically significant at the 5% level based on 2-sided Student's t test.

The increase in air temperature contributed 13.2% to the decrease in runoff and is ranked as the second factor. Both solar radiation and wind speed contributed to the decrease in runoff in opposite manners. In other words, the decreasing solar radiation and wind speed have enhanced runoff via a reduction in the ET, which decreased significantly ($P < 0.027$) during this period. The relative humidity contributed to a small fraction of the change in runoff. The significant increase in atmospheric CO_2 concentration only resulted in a 0.008 mm year^{-2} increase in annual runoff, which is small compared to other climate factors.

Fig. 7 illustrates the spatial distribution of mean annual runoff and its temporal trend. Clearly, the study area can be divided into two regions in terms of the mean annual runoff: (1) a relatively wet region with mean annual runoff >20 mm located in the south and northeast, and (2) a relatively dry region with mean annual runoff <20 mm in the north. In the wet region, the annual runoff decreases significantly, whereas it increases slightly in the dry region. These trends indicate that the spatial distribution of runoff tended to be more homogeneous in the last period over the past 51 years. Overall, a great majority (75%) of the region exhibits a decreasing trend in annual runoff, and 49% of the region exhibits a significant decreasing trend.

In terms of the annual trends caused by the individual factors (Fig. 8), the spatial distributions of the sign of the trends were relatively homogeneous for the air temperature (decreasing), wind speed (increasing), and solar radiation (increasing). The trend caused by precipitation was one of significant decrease in the wet region vs. one of slight increase in the dry region. Although the temporal trend in the atmospheric CO_2 concentration was one of homogeneous increase across the entire region, the

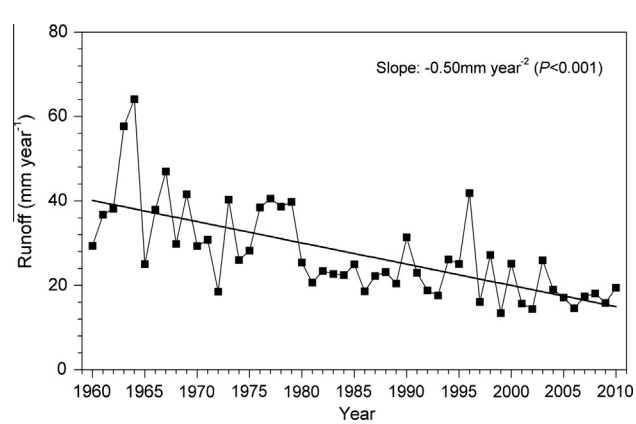

Fig. 6. Interannual variations in the simulated annual runoff.

Table 8
Annual trends in runoff and the relative contribution of each individual factor.

Factors	Slope of annual runoff (mm year^{-2}) (*P*-value)	Contribution (%)
Precipitation	−**0.279** (<0.001)	+55.6
Solar radiation	**0.070** (<0.001)	−13.9
Air temperature	−**0.067** (<0.001)	+13.2
Wind speed	**0.024** (<0.001)	−4.8
Atmospheric CO_2 concentration	**0.008** (<0.001)	−1.6
Relatively humidity	0.004 (0.1809)	−0.8

Bold text indicates that the trend is statistically significant at the 5% level based on 2-sided Student's t test.

response of runoff to this variable was highly spatially heterogeneous. This pattern reflects the complex interactions between the water saving (i.e., stomatal closure) and CO_2 fertilization (i.e., biomass growth stimulation) effects of CO_2 concentration increase. In other words, rising CO_2 concentration enriches the vegetation biomass and thus increases the ET; simultaneously, the rise in CO_2 can reduce the stomatal conductance and thus reduce the ET. Therefore, whether the ET increases or decreases depends on a trade-off between these two counteracting effects.

Fig. 9 shows the dominant factor causing the trend in runoff in each cell. This dominance is determined by the factor that causes the highest rate of change. The trend in annual runoff is primarily due to the change in precipitation in most of the regions (66%), particularly the wet region. The solar radiation and air temperature are dominant factors primarily in the north (17% and 14%, respectively). The wind speed dominates only over a small area in the north (3%). The relative humidity and CO_2 concentration are not considered to be dominant factors across the region.

There are several studies in which the responses of river discharge to the changing climate at different scales were investigated. The resulting impacts of climate change on the trend in runoff were in line with certain of these studies. For example, Yang and Yang (2011) demonstrated that a decline in precipitation was the primary reason for the decline in runoff in the Haihe River basin, based on a climate elasticity approach. Based on a dynamic vegetation and hydrology model, Gerten et al. (2008) reported that precipitation was the primary driver of changes in river discharge over the past century in northern China, whereas the impact of temperature on runoff was negative, and the temperature had a clearly weaker effect than precipitation. The impact of rising atmospheric CO_2 concentration on runoff simulation depends on the mechanisms incorporated into the model. In our study, CLM4 simulations demonstrated a limited enhancement of runoff due to CO_2-induced suppression of transpiration in this region. This result was consistent with that of certain previous studies (Leuzinger and Körner, 2010; Fatichi and Leuzinger, 2013). However, we caution that the effects of rising CO_2 concentration on runoff are still highly uncertain and controversial (Gedney et al., 2006; Huntington, 2008; Davie et al., 2013), and additional mechanisms should be explored.

3.4. Impact of dynamic vegetation phenology on the runoff trend

We further investigated the impacts of dynamic vegetation phenology on the runoff trend by comparing simulations S7 and S8 (Fig. 10). Compared to S8, the interannual variability of runoff in simulation S7 was greatly reduced (74% ($P < 0.05$) of the variability in S8 can be explained by S7), suggesting that simulated vegetation acted as a buffer of climate variability in CLM4. Moreover, the trends in annual runoff in these two simulations differed significantly. In simulation S8, in which the runoff was only determined by changes in the climate forcing (i.e., static vegetation phenology), the magnitude of the decrease in runoff is small (−0.40 mm year^{-2}). When the response of vegetation phenology to the environmental factors (LAI slightly increased during the period, 0.002 year^{-1} ($P = 0.22$)) is included (i.e., S7, dynamic vegetation phenology), the magnitude of the decreasing trend in annual runoff becomes much larger (−0.50 mm year^{-2}). Such a large difference (i.e., 20%) in simulated runoff trends demonstrated that dynamic vegetation phenology may play an important role in predicting the trend in runoff in this region.

Previous studies mentioned earlier focused on evaluating whether the climate or human activities is the dominant factor causing the decreasing trend in annual runoff over the mountainous region of the Haihe River basin. However, one common limitation of these studies was the lack of vegetation dynamics in the models. As demonstrated by our study, the trend in "natural runoff" may be underestimated if dynamic vegetation phenology is

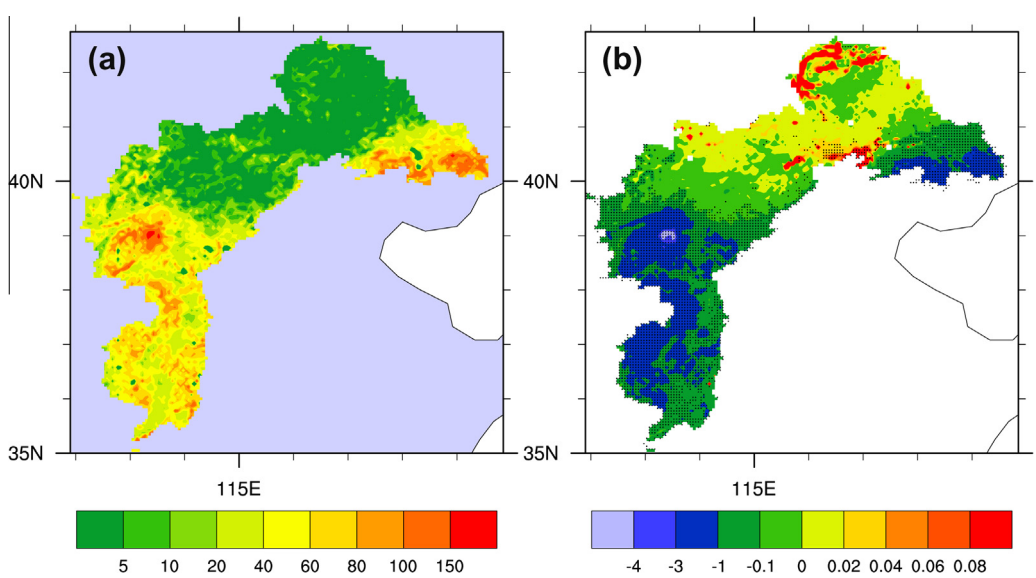

Fig. 7. (a) Simulated mean annual runoff (mm year^{-1}) and (b) trend (mm year^{-2}) in annual runoff. Dot sign in figure (b) indicates that the trend is statistically significant at the 5% level based on 2-sided Student's *t* test.

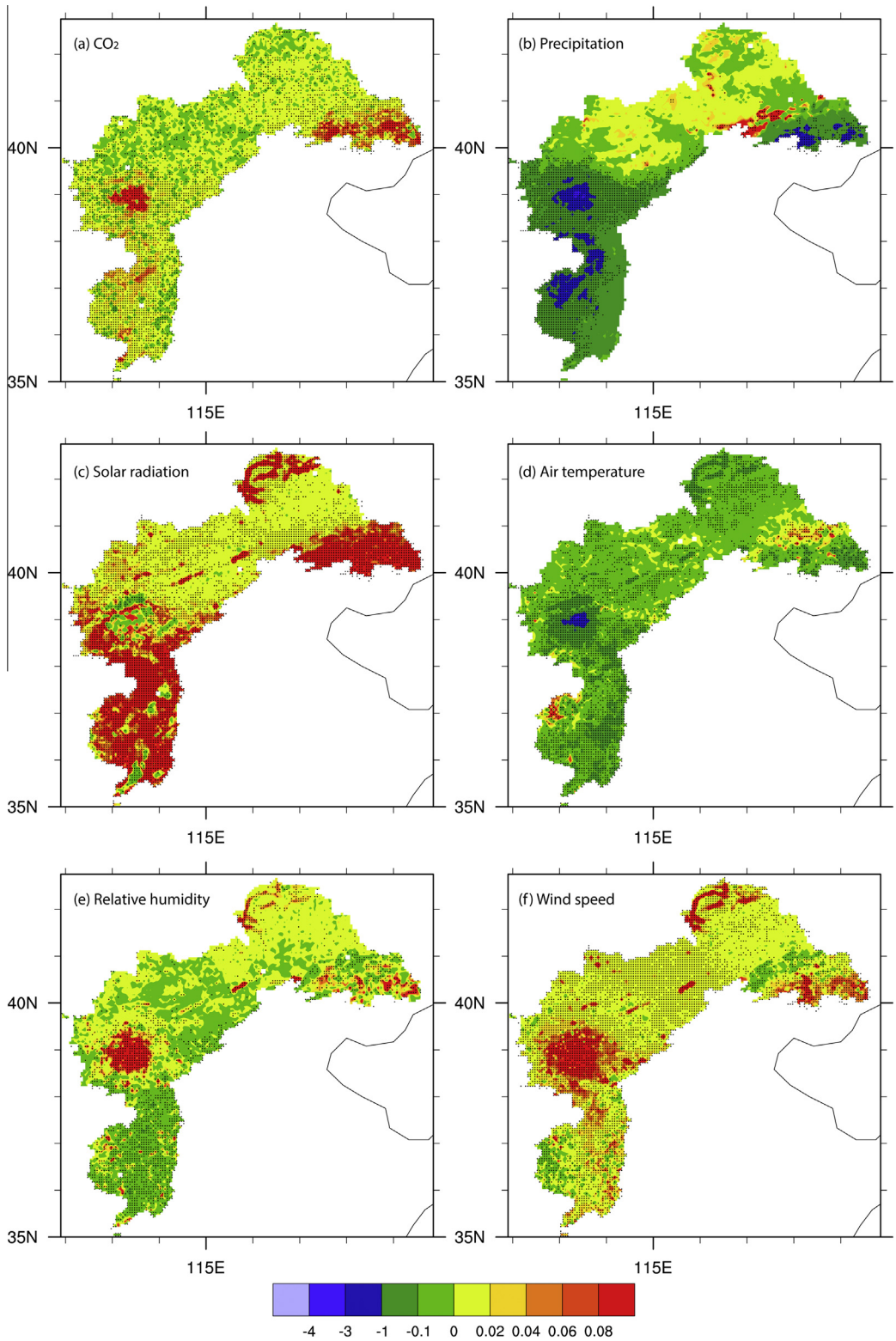

Fig. 8. Trends (mm year^{-2}) in annual runoff caused by individual factors from 1960 to 2010. Dot sign in figures indicates that the trend is statistically significant at the 5% level based on 2-sided Student's *t* test.

neglected in the model, which would then influence directly the diagnosis of the attribution of hydrologic variability.

3.5. Uncertainty and limitations of this study

In this study, the simulation of runoff in the small basins indicated by the NSE was generally poor. We explored the possible reasons and their impacts on runoff simulation, based on the results of the simulations averaged over the six basins. By comparing simulations S7 and D1 (Fig. 11b and Table 9), the R^2 value of the linear regression between the simulated (D1) and observed annual runoff was improved, which indicates that simulation of vegetation LAI can create uncertainty in the interannual variability in the runoff, even though the NSE of simulation S7 was higher than that of

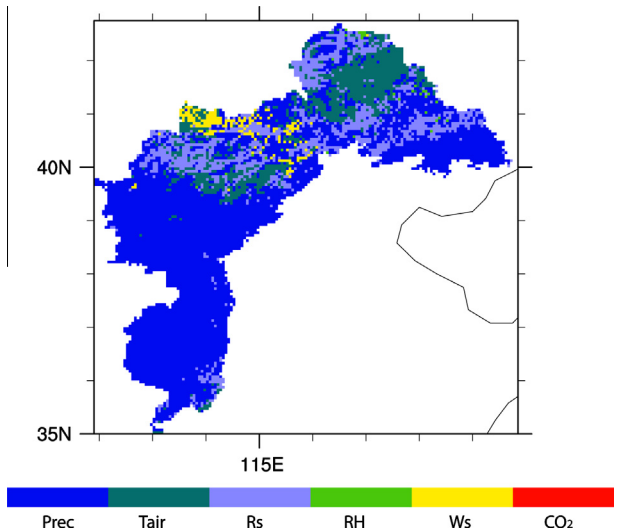

Fig. 9. Dominant driving factors causing annual changes of annual runoff. Prec: precipitation, T_{air}: air temperature, Rs: solar radiation, RH: relative humidity, Ws: wind speed, CO_2: atmospheric CO_2 concentration.

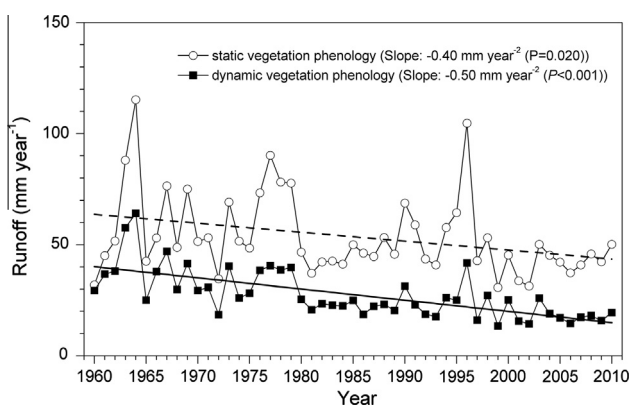

Fig. 10. Impact of vegetation dynamics on the simulated annual runoff.

D1. Compared with D1, the annual runoff simulated by S7 was much lower, which is due to the higher ET induced from the higher simulated LAI by S7 (Fig. 11a). The trends in annual runoff in simulations S7 and D1 also differed, and both simulations displayed biases from the observed trend. The difference between the slopes of the simulated annual runoff in simulations S7 and S8 was larger than that between simulations D1 and S8, suggesting that the simulated response of LAI to changing climate was overemphasised by CLM4. Despite of the bias of the simulated response of LAI to the change in climate in CLM4, the difference between the slopes of annual runoff in D1 and S8 still demonstrates that correct representation of dynamic LAI was important for simulating the trend in runoff. In summary, the simulation of LAI can affect annual runoff in terms of its interannual variability, trend and magnitude, indicating that simulation of vegetation phenology plays an important part in hydrological models in this region. We further compared the simulated contributions to the change in annual runoff by selecting precipitation as an example because the precipitation is the primary contributor to the change in annual runoff. The results indicate that the contribution of precipitation differed by −19% (63% for dynamic LAI to changing precipitation and 78% for static LAI to changing precipitation) between the two approaches (S1 vs. S7 and D1 vs. D2), which further indicates the importance of including the simulation of the response of LAI to changing climate when this type of simulation is conducted.

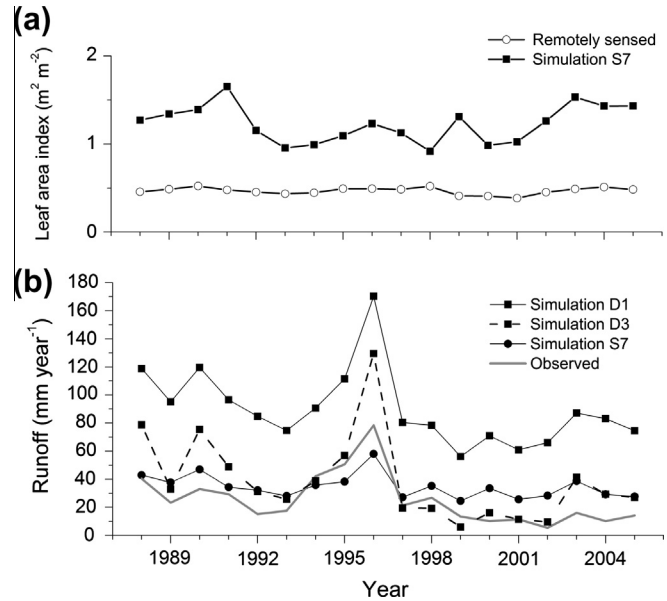

Fig. 11. (a) Interannual variations in simulated and remotely sensed LAI averaged from the 6 basins; (b) comparison of annual runoff simulated by various simulation cases.

Table 9
Statistics of the analysis of uncertainties.

		Mean annual runoff (mm)	Slope of annual runoff (mm year^{-2})	NSE	R^2
Simulation case	S7	35	−0.70	0.29	0.70
	D1	90	−2.37	−12.80	0.82
	D3	39	−2.52	−0.43	0.78
	S8	77	−1.93	−7.85	0.83
Observation		25	−1.53		

Although R^2 was higher in D1 than in S7, the NSE in D1 became even worse when a reliable LAI was prescribed. This result indicated that, except for the simulation of LAI, the poor simulation of runoff primarily attributed to both the hydrological parameters and lower observed river discharge caused by the withdrawal of water during the simulation period (Ma et al., 2010; Wang et al., 2012). In this study, we did not calibrate any parameters related to the hydrological processes primarily because of the data availability. As discussed earlier, there were large uncertainties in simulating the LAI, and thus it is reasonable to calibrate the hydrologic parameters by setting the LAI values using remotely sensed LAI data. However, natural river discharge data were unavailable during the period when remotely sensed LAI data were available (usually beginning in the early 1980s). The disparities between the two datasets indicated the need to improve the simulation of vegetation phenology based on other observations, such as eddy covariance sites (Tan et al., 2010; Fatichi et al., 2012a). Nevertheless, by assuming that the observed values were natural, we tuned the hydrological parameters to determine whether parameter calibration may result in a "better" simulation of the runoff (Fig. 11). By comparing simulations D1 and D3, we observed that tuning the hydrologic parameters can improve the NSE, while this step did not substantially alter the R^2 and the trend in annual runoff (the difference was 6%). These results imply that calibration of the hydrological parameters can change the runoff in terms of its magnitude rather than its interannual variability and trend. Previous studies have also demonstrated that simulations of the runoff and land surface fluxes were sensitive to the hydrology-related

parameters in CLM4 (Hou et al., 2012; Huang et al., 2013), and by calibrating the hydrologic parameters, better performance in runoff and surface flux simulations can be achieved (Sun et al., 2013).

In addition to the uncertainties in the vegetation simulation and model parameters, other uncertainties still remained in our simulations due to limitations in the model setup. First, as mentioned earlier, the meteorological stations are not sufficiently well distributed to represent the spatial variations in the climate over the mountainous area of the Haihe River basin, even though this dataset is the highest quality of available datasets and is commonly used in hydrological studies of this region (e.g., Zheng et al., 2009; Yang and Tian, 2009; Bao et al., 2012; Jia et al., 2012). In particular, the uncertainty in the input precipitation may be the primary reason for the low NSEs in certain small basins discussed earlier. Second, there are still several limitations due to the model structure in CLM4. For example, we assumed that ecosystems in the region were not disturbed by human activities, such as deforestation, reforestation, and grazing, which may have affected the simulation of vegetation phenology. Particularly, crops (the cropland fraction in this region is 33%) were assumed to be C3 grass, which may have had a significant impact on the ET simulation (Lei et al., 2010; Levis et al., 2012). Moreover, uncertainties in root water uptake processes (Li et al., 2013a), bare-soil evaporation formulation (Tang and Riley, 2013), nitrogen limitation effects on hydrological processes (Lee et al., 2013), and representation of soil depth (i.e., a constant soil depth throughout the entire area was used because of the data unavailability), and neglect of the effects of microtopography (e.g., aspect and slope) and micro-meteorological conditions (Fatichi et al., 2012a) can all have possible impacts on hydrological simulations. Additionally, runoff generation and river routing schemes involve several simplifications and assumptions that may affect the simulations of both the runoff magnitude (Li et al., 2011) and seasonality of runoff (Li et al., 2013b). Last, the approach to the sensitivity analysis may contain uncertainty. We assumed that climate factors and CO_2 concentration may vary independently. Such variations may not be true in certain cases. For example, rising CO_2 concentration increases the air temperature through its radiative effect (Cao et al., 2010).

Despite the uncertainties and limitations, our study sheds light in the understanding of the sensitivity of runoff to changes in the various climate forcing variables, particularly the vegetation/biogeochemistry dynamics; we caution that the conclusions in the study are somewhat tied to the data and model used in their current developmental stages. Enhancements in comprehensive observations (such as eddy covariance sites (Lei et al., 2011)) will be crucial for improving the model, and it will prove interesting whether future simulations supported by new observations confirm the results of this study.

4. Conclusions

In this study, we used a process-based model to quantify the relative contributions of climate factor to historical changes in runoff in the mountainous area of the Haihe River basin over the past five decades. Simulated annual runoff in the majority of the region (~75% of the area) exhibited a decreasing trend. Over the entire region, decreasing precipitation and increasing air temperature were found to be the primary and secondary climatic factors driving the decrease in runoff, respectively; whereas decreasing solar radiation and wind speed were the primary and secondary factors offsetting the decreasing runoff. Significantly rising atmospheric CO_2 concentration was found to have a limited impact on changes in runoff. Spatially, precipitation dominates the changes in runoff in most of the region (66%), and the signs of trends caused by solar radiation, wind speed, and air temperature were relatively homogeneous. Compared to the other climate factors, atmospheric CO_2 concentration played a more complex role in driving the interactions between the water and carbon cycles because of the water saving and CO_2 fertilization effects of CO_2 concentration increase. We also determined that dynamic vegetation phenology was critical in modelling the runoff trend, although there was relatively large uncertainty in the simulations of vegetation phenology using CLM4. The decreasing trend in simulated runoff may be underestimated if dynamic vegetation phenology is neglected.

Acknowledgements

This research was supported by the National Natural Science Foundation of China (Project Nos. 51209117 and 51139002) and the National Natural Science Funds for Distinguished Young Scholar (Project No. 51025931). M. Huang is supported by the US Department of Energy Regional and Global Climate Modeling Program through the bilateral agreement between US Department of Energy and China Ministry of Science and Technology on regional climate research. CLM simulations were performed at EMSL, a national scientific user facility sponsored by the Department of Energy's Office of Biological and Environmental Research and located at Pacific Northwest National Laboratory. PNNL is operated for the US DOE by Battelle Memorial Institute under Contract DE-AC05-76RL01830.

References

Bao, Z., Zhang, J., Wang, G., Fu, G., He, R., Yan, X., Jin, J., Liu, Y., 2012. Attribution for decreasing streamflow of the Haihe River basin, northern China: climate variability or human activities? J. Hydrol. 460–461, 117–129.

Bonan, G.B., Levis, S., Kergoat, L., Oleson, K.W., 2002. Landscapes as patches of plant functional types: an integrating concept for climate and ecosystem models. Global Biogeochem. Cycles 16 (2), 1021.

Branstetter, M.L., Erickson III, D.J., 2003. Continental runoff dynamics in the Community Climate System Model 2 (CCSM2) control simulation. J. Geophys. Res. 108 (D17), 4550. http://dx.doi.org/10.1029/2002JD003212.

Cao, L., Bala, G., Caldeira, K., Nemani, R., Ban-Weiss, G., 2010. Importance of carbon dioxide physiological forcing to future climate change. Proc. Natl. Acad. Sci. USA 107 (21), 9513–9518.

Cong, Z., Yang, D., Gao, B., Yang, H., Hu, H., 2009. Hydrological trend analysis in the Yellow River basin using a distributed hydrological model. Water Resour. Res. 45, W00A13. http://dx.doi.org/10.1029/2008WR006852.

Dan, L., Ji, J., Xie, Z., Chen, F., Wen, G., Richey, J.E., 2012. Hydrological projections of climate change scenarios over the 3H region of China: a VIC model assessment. J. Geophys. Res. 117, D11102. http://dx.doi.org/10.1029/2011JD017131.

Davie, J.C.S., Falloon, P.D., Kahana, R., Dankers, R., Betts, R., Portmann, F.T., Wisser, D., et al., 2013. Comparing projections of future changes in runoff from hydrological and biome models in ISI-MIP. Earth Syst. Dynam. 4 (2), 359–374.

de Jong, R., de Bruin, S., de Wit, A., Schaepman, M.E., Dent, D.L., 2011. Analysis of monotonic greening and browning trends from global NDVI time-series. Remote Sens. Environ. 115, 692–702.

Dentener, F., Drevet, J., Lamarque, J.F., Bey, I., Eickhout, B., Fiore, A.M., Hauglustaine, D., Horowitz, L.W., Krol, M., Kulshrestha, U.C., et al., 2006. Nitrogen and sulfur deposition on regional and global scales: a multimodel evaluation. Global Biogeochem. Cycles 20, GB4003. http://dx.doi.org/10.1029/2005GB002672.

Donohue, R.J., Roderick, M.L., McVicar, T.R., 2012. Roots, storms and soil pores: incorporating key ecohydrological processes into Budyko's hydrological model. J. Hydrol. 436–437, 35–50.

Edwards, E.J., Osborne, C.P., Strömberg, C.A., Smith, S.A., 2010. The origins of C4 grasslands: integrating evolutionary and ecosystem science. Science. 328 (5978), 587–591.

Fatichi, S., Leuzinger, S., 2013. Reconciling observations with modeling: the fate of water and carbon allocation in a mature deciduous forest exposed to elevated CO_2. Agric. For. Meteorol. 174 (175), 144–157. http://dx.doi.org/10.1016/j.agrformet.2013.02.005.

Fatichi, S., Ivanov, V.Y., Caporali, E., 2012a. A mechanistic ecohydrological model to investigate complex interactions in cold and warm water-controlled environments. 1. Theoretical framework and plot-scale analysis. J. Adv. Model. Earth Syst. 4, M05002. http://dx.doi.org/10.1029/2011MS000086.

Fatichi, S., Ivanov, V.Y., Caporali, E., 2012b. A mechanistic ecohydrological model to investigate complex interactions in cold and warm water-controlled environments. 2. Spatiotemporal analyses. J. Adv. Model. Earth Syst. 4, M05003. http://dx.doi.org/10.1029/2011MS000087.

Gedney, N., Cox, P.M., Betts, R.A., Boucher, O., Huntingfor, C., Stott, P.A., 2006. Detection of a direct carbon dioxide effect in continental river runoff records. Nature 439 (16), 835–838.

Gerten, D., Rost, S., von Bloh, W., Lucht, W., 2008. Causes of change in 20th century global river discharge. Geophys. Res. Lett. 35, L20405. http://dx.doi.org/10.1029/2008GL035258.

Gupta, H.V., Kling, H., Yilmaz, K.K., Martinez, G.F., 2009. Decomposition of the mean squared error and NSE performance criteria: implications for improving hydrological modeling. J. Hydrol. 377, 80–91.

Haihe River Commission, 2013. <http://www.hwcc.gov.cn/pub/hwcc/static/lygk/qxsw.htm>.

Hou, Z., Huang, M., Leung, L.R., Lin, G., Ricciuto, D.M., 2012. Sensitivity of surface flux simulations to hydrologic parameters based on an uncertainty quantification framework applied to the Community Land Model. J. Geophys. Res. 117, D15108. http://dx.doi.org/10.1029/2012JD017521.

Huang, M., Hou, Z., Leung, L.R., Ke, Y., Liu, Y., Fang, Z., Sun, Y., 2013. Uncertainty analysis of runoff simulations and parameter identifiability in the community land model – evidence from MOPEX basins. J. Hydrometeor.. http://dx.doi.org/10.1175/JHM-D-12-0138.1.

Huntington, T.G., 2008. CO2-induced suppression of transpiration cannot explain increasing runoff. Hydrol. Process. 22, 311–314.

IPCC AR4 WG1, 2007, in Solomon, S., Qin, D., Manning, M., Chen, Z., Marquis, M., Averyt, K.B., Tignor, M., Miller, H.L., Climate Change 2007: The Physical Science Basis, Contribution of Working Group I to the Fourth Assessment Report of the Intergovernmental Panel on Climate Change, Cambridge University Press.

Ivanov, V.Y., Bras, R.L., Vivoni, E.R., 2008. Vegetation-hydrology dynamics in complex terrain of semiarid areas: II. Energy-water controls of vegetation spatio-temporal dynamics and topographic niches of favorability. Water Resour. Res. 44, W03430. http://dx.doi.org/10.1029/2006WR005595.

Jackson, T.L., Feddema, J.J., Oleson, K.W., Bonan, G.B., Bauer, J.T., 2010. Parameterization of urban characteristics for global climate modeling. Ann. Assoc. Am. Geogr. 100 (4), 848–865.

Jia, Y., Ding, X., Wang, H., Zhou, Z., Qiu, Y., Niu, C., 2012. Attribution of water resources evolution in the highly water-stressed Hai River Basin of China. Water Resour. Res. 48, W02513. http://dx.doi.org/10.1029/2010WR009275.

Lawrence, D., Oleson, K.W., Flanner, M.G., Thorton, P.E., Swenson, S.C., Lawrence, P.J., Zeng, X., Yang, Z.-L., Levis, S., Skaguchi, K., Bonan, G.B., Slater, A.G., 2011. Parameterization improvements and functional and structural advances in version 4 of the Community Land Model. J. Adv. Model. Earth Syst. 3, M03001, 27, doi: http://dx.doi.org/10.1029/2011MS000045.

Lee, E., Felzer, B.S., Kothavala, Z., 2013. Effects of nitrogen limitation on hydrological processes in CLM4-CN. J. Adv. Model. Earth Syst. 5. http://dx.doi.org/10.1002/jame.20046.

Lei, H., Yang, D., Lokupitiya, E., Shen, Y., 2010. Coupling land surface and crop growth models for predicting evapotranspiration and carbon exchange in wheat-maize rotation croplands. Biogeosciences 7, 3363–3375.

Lei, H., Yang, D., Shen, Y., Liu, Y., Zhang, Y., 2011. Simulation of evapotranspiration and carbon dioxide flux in the wheat-maize rotation croplands of the North China Plain using the Simple Biosphere Model. Hydrol. Process. 25, 3107–3120.

Lei, H., Yang, D., Cai, J., Wang, F., 2013. Long-term variability of the carbon balance in a large irrigated area along the lower Yellow River from 1984 to 2006. Sci. China Earth Sci. 56, 671–683.

Leuzinger, S., Körner, C., 2010. Rainfall distribution is the main driver of runoff under future CO_2-concentration in a temperate deciduous forest. Global Change Biol. 16, 246–254, doi: 10.1111/j.1365-2486.2009.01937.x.

Levis, S., Bonan, G.B., Kluzek, E., Thornton, P.E., Jones, A., Sacks, W.J., Kucharik, C.J., 2012. Interactive crop management in the Community Earth System Model (CESM1): seasonal influences on land-atmosphere fluxes. J. Clim. 25 (14), 4839–4859.

Li, H., Huang, M., Wigmosta, M.S., Ke, Y., Coleman, A.M., Leung, L.R., Wang, A., Ricciuto, D.M., 2011. Evaluating runoff simulations from the Community Land Model 4.0 using observations from flux towers and a mountainous watershed. J. Geophys. Res. 116, D24120. http://dx.doi.org/10.1029/2011JD016276.

Li, L., van der tol, C., Chen, X., Jing, C., Su, B., Luo, G., Tian, X., 2013a. Representing the root water uptake process in the Common Land Model for better simulating the energy and water vapour fluxes in a Central Asian desert ecosystem. J. Hydrol. 502, 145–155.

Li, H.-Y., Wigmosta, M.S., Wu, H., Huang, M., Ke, Y., Coleman, A.M., Leung, L.R., 2013b. A physically based runoff routing model for land surface and earth system models. J. Hydrometeor. 14, 808–828.

Li, Q., Ishidaira, H., 2012. Development of a biosphere hydrological model considering vegetation dynamics and its evaluation at basin scale under climate change. J. Hydrol. 412–413, 3–13.

Li, D., Pan, M., Cong, Z., Zhang, L., Wood, E., 2013. Vegetation control on water and energy balance within the Budyko framework. Water Resour. Res. 49. http://dx.doi.org/10.1002/wrcr.20107.

Liu, C., Xia, J., 2004. Water problems and hydrological research in the Yellow River and the Huai and Hai River basins of China. Hydrol. Process. 18, 2197–2210.

Liu, J., Liu, M., Tian, H., Zhuang, D., Zhang, Z., Zhang, W., Tang, X., Deng, X., 2005. Spatial and temporal patterns of China's cropland during 1990–2000: an analysis based on Landsat TM data. Remote Sens. Environ. 98, 442–456.

Liu, Y., Liu, R., Chen, J.M., 2012. Retrospective retrieval of long-term consistent global leaf area index (1981–2011) from combined AVHRR and MODIS data. J. Geophys. Res. 117, G04003. http://dx.doi.org/10.1029/2012JG002084.

Lucht, W., Prentice, I.C., Myneni, R.B., Sitch, S., Friedlingstein, P., Cramer, W., Bousquet, P., Buermann, W., Smith, B., 2002. Climatic control of the high-latitude vegetation greening trend and pinatubo effect. Science 296, 1687–1689.

Ma, H., Yang, D., Tan, S.K., Gao, B., Hu, Q., 2010. Impact of climate variability and human activity on streamflow decrease in the Miyun Reservoir catchment. J. Hydrol. 389, 317–324.

Mao, J.F., Thornton, P.E., Shi, X.-Y., Zhao, M., Post, W.M., 2012. Remote sensing evaluation of CLM4 GPP for the period 2000–09. J. Clim. 25, 5327–5342.

Murray, S.J., Watson, I.M., Prentice, I.C., 2013. The use of dynamic global vegetation models for simulating hydrology and the potential integration of satellite observations. Prog. Phys. Geogr. 37, 63–97.

Oleson, K.W., Lawrence, D.M., Bonan, G.B., Flanner, M.G., Kluzek, E., Lawrence, P.J., Levis, S., Swenson, S.C., Thornton, P.E., Dai, A., Decker, M., Dickinson, R., Feddema, J., Heald, C.L., Hoffman, F., Lamarque, J.-F., Mahowald, N., Niu, G.-Y., Qian, T., Randerson, J., Running, S., Sakaguchi, K., Slater, A., Stockli, R., Wang, A., Yang, Z.-L., Zeng, X., Zeng, X., 2010. Technical description of version 4.0 of the Community Land Model (CLM). NCAR Technical Note NCAR/TN-478+STR, National Center for Atmospheric Research, Boulder, CO, p. 257.

Peng, S., Liu, W., Wang, W., Shao, Q., Jiao, X., Yu, Z., Xing, W., Xu, J., Zhang, Z., Luo, Y., 2013. Estimating the effects of climatic variability and human activities on streamflow in the Hutuo River basin, China. J. Hydrol. Eng. 18 (4), 422–430.

Piao, S., Ciais, P., Huang, Y., Shen, Z., Peng, S., Li, J., Zhou, L., Liu, H., Ma, Y., Ding, Y., Friedlingstein, P., Liu, C., Tan, K., Yu, Y., Zhang, T., Fang, J., 2010. The impacts of climate change on water resources and agriculture in China. Nature 467, 43–51.

Piao, S., Friedlingstein, P., Ciais, P., Zhou, L., Chen, A., 2006. Effect of climate and CO_2 changes on the greening of the Northern Hemisphere over the past two decades. Geophys. Res. Lett. 33, L23402. http://dx.doi.org/10.1029/2006GL028205.

Piao, S., Tan, K., Nan, H., Ciais, P., Fang, J., Wang, T., Vuichard, N., Zhu, B., 2012. Impacts of climate and CO2 changes on the vegetation growth and carbon balance of Qinghai-Tibetan grasslands over the past five decades. Glob. Planet. Change. 98–99, 73–80.

Pitman, A.J., 2003. The evolution of, and revolution in, land surface schemes designed for climate models. Int. J. Climatol. 23 (5), 479–510.

Roderick, M.L., Farquhar, G.D., 2002. The cause of decreased pan evaporation over the past 50 years. Science 298, 1410–1411.

Rodriguez-Iturbe, I., 2000. Ecohydrology: a hydrologic perspective of climate-soil-vegetation dynamics. Water Resour. Res. 36 (1), 3–9.

Sakaguchi, K., Zeng, X., Christoffersen, B.J., Restrepo-Coupe, N., Saleska, S.R., Brando, P.M., 2011. Natural and drought scenarios in an east central Amazon forest: Fidelity of the Community Land Model 3,5 with three biogeochemical models. J. Geophys. Res. 116, G01029. http://dx.doi.org/10.1029/2010JG001477.

Shangguan, W., Dai, Y., Liu, B., Ye, A., Yuan, H., 2012. A soil particle-size distribution dataset for regional land and climate modelling in China. Geoderma 171–172, 85–91.

Shen, C., Niu, J., Phanikumar, M.S., 2013. Evaluating controls on coupled hydrologic and vegetation dynamics in a humid continental climate watershed using a subsurface – land surface processes model. Water Resour. Res. doi: 10.1002/wrcr.20189, in press.

Shi, X., Mao, J., Thornton, P.E., Huang, M., 2013. Spatiotemporal patterns of evapotranspiration in response to multiple environmental factors simulated by the Community Land Model. Environ. Res. Lett. 8, 024012, p. 12.

Shi, X., Mao, J., Thorton, P.E., Hoffman, F.O., Post, W.M., 2011. The impact of climate CO_2, nitrogen deposition and land use change on simulated contemporary global river flow. Geophys. Res. Lett. 38, L08704. http://dx.doi.org/10.1029/2011GL046773.

Stöckli, R., Lawrence, D.M., Niu, G.-Y., Oleson, K.W., Thornton, P.E., Yang, Z.-L., Bonan, G.B., Denning, A.S., Running, S.W., 2008. Use of FLUXNET in the Community Land Model development. J. Geophys. Res. 113, G01025. http://dx.doi.org/10.1029/2007JG000562.

Sun, C., Ren, L., 2013. Assessment of surface water resources and evapotranspiration in the Haihe River basin of China using SWAT model. Hydrol. Process. 27, 1200–1222.

Sun, Y., Hou, Z., Huang, M., Tian, F., Leung, L.R., 2013. Inverse modeling of hydrologic parameters using surface flux and runoff observations in the Community Land Model. Hydrol. Earth Syst. Sci. Discuss. 10, 5077–5119. http://dx.doi.org/10.5194/hessd-10-5077-2013.

Tague, C.L., Band, L.E., 2004. RHESSys: regional hydro-ecologic simulation system: an object-oriented approach to spatially distributed modeling of carbon, water, and nutrient cycling. Earth Interact. 8 (19), 1–42.

Tan, K., Ciais, P., Piao, S., Wu, X., Tang, Y., Vuichard, N., Liang, S., Fang, J., 2010. Application of the ORCHIDEE global vegetation model to evaluate biomass and soil carbon stocks of Qinghai-Tibetan grasslands. Global Biogeochem. Cycles. 24, GB1013. http://dx.doi.org/10.1029/2009GB003530.

Tang, J., Riley, W.J., 2013. Impacts of a new bare-soil evaporation formulation on site, regional, and global surface energy and water budgets in CLM4. J. Adv. Model. Earth Syst. 5, 558–571. http://dx.doi.org/10.1002/jame.20034.

Thornton, P.E., Rosenbloom, N.A., 2005. Ecosystem model spin-up: estimating steady state conditions in a coupled terrestrial carbon and nitrogen cycle model. Ecol. Model. 189, 25–48.

Wada, Y., van Beek, L.P.H., van Kempen, C.M., Reckman, J.W.T.M., Vasak, S., Bierkens, M.F.P., 2010. Global depletion of groundwater resources. Geophys. Res. Lett. 37, L20402. http://dx.doi.org/10.1029/2010GL044571.

Wang, A., Zeng, X., 2011. Sensitivities of terrestrial water cycle simulations to the variations of precipitation and air temperature in China. J. Geophys. Res. 116, D02107. http://dx.doi.org/10.1029/2010JD014659.

Wang, L., Koike, T., Yang, K., Jackson, T.J., Bindlish, R., Yang, D., 2009. Development of a distributed biosphere hydrological model and its evaluation with the

Southern Great Plains Experiments (SGP97 and SGP99). J. Geophys. Res. 114, D08107. http://dx.doi.org/10.1029/2008JD010800.
Wang, W., Peng, S., Yang, T., Shao, Q., Xu, J., Xing, W., 2011. Spatial and temporal characteristics of reference evapotranspiration trends in the Haihe River basin. China. J. Hydrol. Eng. 16 (3), 239–252.
Wang, W., Shao, Q., Yang, T., Peng, S., Xing, W., Sun, F., Luo, Y., 2012. Quantitative assessment of the impact of climate variability and human activities on runoff changes: a case study in four catchments of the Haihe River basin, China. Hydrol. Process., doi: 10.1002/hyp.9299.
Wu, H., Kimball, J.S., Li, H., Huang, M., Leung, L.R., Adler, R.F., 2012. A new global river network database for macroscale hydrologic modeling. Water Resour. Res. 48, W09701. http://dx.doi.org/10.1029/2012WR012313.
Yang, D., Li, C., Hu, H., Lei, Z., Yang, S., Kusuda, T., Koike, T., Musiake, K., 2004. Analysis of water resources variability in the Yellow River of China during the last half century using historical data. Water Resour. Res. 40, W06502. http://dx.doi.org/10.1029/2003WR002763.
Yang, D., Sun, F., Liu, Z., Cong, Z., Ni, G., Lei, Z., 2007. Analyzing spatial and temporal variability of annual water-energy balance in nonhumid regions of China using the Budyko hypothesis. Water Resour. Res. 43, W04426. http://dx.doi.org/10.1029/2006WR005224.
Yang, D., Shao, W., Yeh, P.J.-F., Yang, H., Kanae, S., Oki, T., 2009. Impact of vegetation coverage on regional water balance in the nonhumid regions of China. Water Resour. Res. 45, W00A14. http://dx.doi.org/10.1029/2008WR006948.
Yang, H., Yang, D., 2011. Derivation of climate elasticity of runoff to assess the effects of climate change on annual runoff. Water Resour. Res. 47, W07526. http://dx.doi.org/10.1029/2010WR009287.
Yang, H., Yang, D., 2012. Climatic factors influencing changing pan evaporation across China from 1961 to 2001. J. Hydrol. 414–415, 184–193.
Yang, K., Koike, T., 2005. A general model to estimate hourly and daily solar radiation for hydrological studies. Water Resour. Res. 41, W10403. http://dx.doi.org/10.1029/2005WR003976.
Yang, Y., Tian, F., 2009. Abrupt change of runoff and its major driving factors in Haihe River Catchment, China. J. Hydrol. 374, 373–383.
Zhang, K., Kimball, J.S., Nemani, R.R., Running, S.W., 2010. A continuous satellite-derived global record of land surface evapotranspiration from 1983 to 2006. Water Resour. Res. 46, W09522. http://dx.doi.org/10.1029/2009WR008800.
Zhao, M., Heinsch, F.A., Nemani, R.R., Running, S.W., 2005. Improvements of the MODIS terrestrial gross and net primary production global data set. Remote Sens. Environ. 95, 164–176.
Zhao, M., Running, S.W., Nemani, R.R., 2006. Sensitivity of Moderate Resolution Imaging Spectroradiometer (MODIS) terrestrial primary production to the accuracy of meteorological reanalyses. J. Geophys. Res. 111, G01002. http://dx.doi.org/10.1029/2004JG000004.
Zheng, H., Liu, X., Liu, C., Dai, X., Zhu, R., 2009. Assessing contributions to panevaporation trends in Haihe River Basin, China. J. Geophys. Res. 114, D24105. http://dx.doi.org/10.1029/2009JD012203.